133–135 °C [lit.[12] 137–137.7 °C]; ^{1}H NMR (CDCl$_3$) δ 6.4 (m, 2, vinyl), 5.02 (m, 2, bridgehead), 4.65 (s, 2, H2 and H3).

**cis,endo-7-Oxabicyclo[2.2.1]heptane-2,3-diol.** A mixture of the cis,-endo carbonate (1.8 g, 0.012 mol), 0.4 g of 10% Pd on C, and 100 mL of ethanol was stirred in a H$_2$ atmosphere until the theoretical amount of H$_2$ was taken up. The catalyst was removed by filtration, and the filtrate was concentrated. The residue was treated with 50 mL of 5% NaOH, and the mixture was shaken until all the solid had dissolved. The solution was then neutralized with concentrated HCl. Continuous ether extraction for 4 days gave the crude diol, which was recrystallized from benzene/hexane to give 1.23 g (81%) of the desired diol: mp 148–150 °C; ^{1}H NMR (CDCl$_3$) δ 4.47 (br s, 2, bridgehead), 3.94 (br s, 2, H2 and H3), 2.8 (very br s, 2, OH), 2.05–1.23 (m, 4, methylene). Anal. Calcd for C$_6$H$_{10}$O$_3$: C, 55.37; H, 7.74. Found: C, 54.88; H, 7.73.

**cis,endo-7-Oxabicyclo[2.2.1]hepta-2,3-diyl Dibrosylate (6).** The cis,endo diol was treated with brosyl chloride by the above procedure to give a 60% yield of the desired dibrosylate: mp 179–181 °C; ^{1}H NMR (CDCl$_3$) δ 7.8 (narrow ABq, 8, aromatic), 4.6–4.45 (m, 4, bridgehead, H2, and H3), 2.1–1.5 (m, 4, methylene). Anal. Calcd for C$_{18}$H$_{16}$Br$_2$S$_2$O$_7$: C, 38.05; H, 2.84. Found: C, 37.83; H, 2.72.

**cis,endo-7-Oxabicyclo[2.2.1]hepta-2,3-diyl Diacetate.** The cis,endo diol was treated with Ac$_2$O by the above procedure to give an analytical sample of the diacetate as a clear liquid: ^{1}H NMR (CDCl$_3$) δ 4.85 (m, 2, H2 and H3), 4.65 (m, 2, bridgehead), 2.05 (s, 6, CH$_3$), 2.0–1.55 (m, 4, methylene).

**cis,exo-7-Oxabicyclo[2.2.1]heptane-2,3-diol** was prepared from the cis,exo carbonate by the same procedure used to prepare the cis,endo isomer, except that the cis,exo diol could not be recovered by ether extraction. Instead, after neutralization, the H$_2$O was removed by rotary evaporation at reduced pressure, and the residue was treated with warm CH$_2$Cl$_2$. The crude diol was obtained by filtration and concentration of the filtrate in nearly quantitative yield. Recrystallization from benzene afforded the diol as a white solid: mp 77–79 °C; ^{1}H NMR (CDCl$_3$) δ 4.35 (m, 2, bridgehead), 3.84 (s, 2, H2 and H3), 3.4 (s, 2, OH), 1.85–1.2 (m, 4, methylene). Anal. Calcd for C$_6$H$_{10}$O$_3$: C, 55.37; H, 7.74. Found: C, 55.29; H, 7.57.

**cis,exo-7-Oxabicyclo[2.2.1]hepta-2,3-diyl Dibrosylate (7).** The diol was treated with brosyl chloride by the above procedure to give the desired dibrosylate in 82% yield: mp 169–170 °C; ^{1}H NMR (CDCl$_3$) δ 7.8 (narrow ABq, 8, aromatic), 4.75 (s, 2, H2 and H3), 4.60 (m, 2, bridgehead), 1.85–1.40 (m, 4, methylene). Anal. Calcd for C$_{18}$H$_{16}$Br$_2$S$_2$O$_7$: C, 38.05; H, 2.84. Found: C, 37.89; H, 2.77.

**cis,exo-7-Oxabicyclo[2.2.1]hepta-2,3-diyl Diacetate.** Treatment of the cis,exo diol with excess Ac$_2$O by the above procedure produced an analytical sample of the desired diacetate as a clear liquid: ^{1}H NMR (CDCl$_3$) δ 4.88 (s, 2, H2 and H3), 4.51 (m, 2, bridgehead), 2.08 (s, 6, CH$_3$), 1.80–1.45 (m, 4, methylene).

**3-Formylcyclopentyl acetate** was isolated by preparative GC from the product mixture of the endo brosylate 6 and the exo brosylate 7: ^{1}H NMR (CDCl$_3$) δ 9.75 (s, 1), 5.22 (m, 1), 2.2–1.3 (m, 7), 2.04 (s, 3).

# Photochemistry of Iron Atoms and Dimers with Ethylene in Cryogenic Matrices. The FTIR Spectrum of Ethenyliron Hydride

**Zakya H. Kafafi,\* Robert H. Hauge, and John L. Margrave**

*Contribution from the Department of Chemistry and Rice Quantum Institute, Rice University, Houston, Texas 77251. Received June 3, 1985*

**Abstract:** Evidence from infrared studies shows that atomic and molecular iron interact with ethylene in two distinct ways. One type of interaction leads to the formation of the classical known for many transition metal/ethylene systems. In this context we have isolated Fe(C$_2$H$_4$)$_n$, where $n \geq 2$, as well as Fe$_2$(C$_2$H$_4$)$_m$, where $m = 1$, 2 in solid inert gas matrices. Another type of interaction deduced from the present study takes place between one or more of the hydrogen atoms of ethylene and atomic iron. Two forms of a hydrogen-bonded complex exhibit a slightly perturbed ethylene-like infrared spectrum. Perturbations on all the ethylene infrared active modes have been measured. A photoreversible oxidative-addition/reductive-elimination reaction of the form

$$Fe(C_2H_4) \underset{\lambda \geq 400 \text{ nm}}{\overset{280-360 \text{ nm}}{\rightleftharpoons}} HFeC_2H_3$$
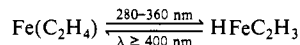
has been observed at 14 K in solid argon and krypton. One of the hydrogen-bonded complexes, Fe(C$_2$H$_4$), was found to be the primary precursor for formation of the insertion product, HFeC$_2$H$_3$. Frequencies of ten fundamental modes of HFeC$_2$H$_3$, HFe$^{13}$C$_2$H$_3$, and DFeC$_2$D$_3$ have been measured in the 450–4000 cm$^{-1}$ infrared region.

The interactions between transition metals and ethylene have been known since the discovery of Zeise's salt in 1831.[1] Recently many studies[2–18] have concentrated on the interaction between

zerovalent transition metals and ethylene in cryogenic matrices. The synthesis of triethylene–nickel[19] has spurred many theoreticians to attempt to understand the type of bonding that exists between zerovalent transition metals and ethylene as well as to predict the geometry of this new class of π-complexes.[20–24] The

(1) Zeise, W. C.; Pogg *Ann.* **1831**, *21*, 497.
(2) Parker, S. F.; Peden, C. H. F.; Barnett, P. H.; Pearson, R. G. *Inorg. Chem.* **1983**, *22*, 2813.
(3) Kasai, P. H. *J. Am. Chem. Soc.* **1983**, *105*, 6704.
(4) McIntosh, D. F.; Ozin, G. A.; Messmer, R. P. *Inorg. Chem.* **1980**, *19*, 3321.
(5) Kasai, P. H.; McLeod, D., Jr.; Watanabe, T. *J. Am. Chem. Soc.* **1980**, *102*, 179.
(6) Ozin, G. A.; Power, W. J.; Upton, T. H.; Goddard, W. A., III *J. Am. Chem. Soc.*, **1978**, *100*, 4750.
(7) Lee Hanlan, A. J.; Ozin, G. A.; Power, W. J. *Inorg. Chem.* **1978**, *17*, 3648.
(8) Ozin, G. A.; Power, W. J. *Inorg. Chem.* **1978**, *17*, 2836.
(9) Lee Hanlan, A. J.; Ozin, G. A. *Ber. BunsenGes. Phys. Chem.* **1978**, *82*, 101.

(10) Ozin, G. A. *Acc. Chem. Res.* **1977**, *10*, 21.
(11) Ozin, G. A.; Huber, H.; McIntosh, D. *Inorg. Chem.* **1977**, *16*, 3070.
(12) Ozin, G. A.; Power, W. J. *Inorg. Chem.* **1977**, *16*, 212.
(13) Huber, H.; Ozin, G. A.; Power, W. J. *Inorg. Chem.* **1977**, *16*, 979.
(14) McIntosh, D.; Ozin, G. A. *J. Organomet. Chem.* **1976**, *121*, 127.
(15) Huber, H.; Ozin, G. A.; Power, W. J. *J. Am. Chem. Soc.* **1976**, *98*, 6508.
(16) Huber, H.; McIntosh, D.; Ozin, G. A. *J. Organomet. Chem.* **1976**, *112*, C50.
(17) Kasai, P. H.; McLeod, D., Jr. *J. Am. Chem. Soc.* **1975**, *97*, 6602.
(18) Kasai, P. H. *J. Am. Chem. Soc.* **1983**, *105*, 6704.
(19) Fischer, K.; Jonas, K.; Wilke, G. *Angew. Chem.* **1973**, *85*, 620; *Angew. Chem., Int. Ed. Engl.* **1973**, *12*, 565.
(20) Rosch, N.; Hoffmann, R. *Inorg. Chem.* **1974**, *13*, 2656.

accepted interaction in these metal–olefin systems follows the classical Dewar–Chatt–Duncanson model[25,26] where the ethylene molecule interacts with the metal both as a $\sigma$-donor through the (C=C) $\pi$-orbital and a $\pi$-acceptor through the (C=C) $\pi^*$-orbital.

A recent matrix isolation infrared and Mössbauer study[2] reported the formation of the $\pi$-complexes $Fe(C_2H_4)$, $Fe_2(C_2H_4)$, and $Fe_2(C_2H_4)_2$, for the mono- and diiron/ethylene reactions. Broad-band irradiation of the matrix caused the unreacted iron atoms, observed in neat ethylene, to react with ethylene and form $Fe(C_2H_4)$. In the present paper we present the first evidence for the formation of a hydrogen-bonded transition-metal ethylene complex as well as the classical $\pi$-complex in cryogenic matrices. We further show that this hydrogen-bonded complex is photoactivated via ultraviolet light and rearranges to yield vinyliron hydride. This insertion product will further undergo reductive-elimination when excited by visible irradiation ($\lambda \geq 400$ nm) and return to the initial hydrogen-bonded complex, monoethylene–iron. The present study will also demonstrate that the complexes recently identified as "$Fe_n(C_2H_4)$"[2] are actually $Fe_n(C_2H_4)_m$ where $n = 1, 2$ and $m \geq 2$. This conclusion was based on ethylene concentration as well as mixed-isotope ($^{12}C_2H_4/^{13}C_2H_4$) studies.

## Experimental Section

A new multisurface matrix isolation apparatus[27] interfaced to the IBM FTIR, Model IR98, has been used in this study. Sixty polished rhodium-plated copper surfaces are available for deposition experiments. These multiple reflection surfaces allow convenient, efficient, and rapid study of the effects of different experimental parameters such as the type of matrix, the matrix-to-reactant ratio, the isotopic ratio, the metal-deposition rate, and the wavelength range used in the broad band selective filter photolysis studies. Three quartz crystal microbalances have been mounted directly on the block allowing a precise measure of the molar ratios of metal, reactant, and matrix gases. The rotatable-translational matrix block lies on top of the stationary closed cycle helium refrigerator, an Air Products Displex Model CSW-202. Temperatures in the range of 13.5–15 K were used in this new system. A room-temperature water-cooled quartz crystal microbalance is situated at the back of the metal furnace allowing constant monitoring of the rate of metal deposition.

In a typical experiment iron was placed in an alumina crucible and heated slowly in vacuo at 1000 °C for a period of a few hours. After we measured the rates of deposition of iron, ethylene, and argon and determined their molar ratios, the deposition experiment took place for a period of 30 min. The block was then rotated 180°, and a single-beam Fourier transform infrared spectrum of the matrix was measured at a 1-cm$^{-1}$ resolution. A double-beam spectrum was achieved by ratioing the single-beam matrix spectrum to that of a clean matrix surface. For a better signal-to-noise ratio the number of scans was sometimes increased from 100 to 1000 scans. In some cases spectra were obtained at higher resolutions (0.25–0.5 cm$^{-1}$). Matrices were usually irradiated subsequent to deposition. The radiation source used was a 100 W medium-pressure short-arc mercury lamp which was focused to a 2 cm diameter spot on the matrix surface. A water Pyrex filter with various Corning long-pass cutoff filters was used for wavelength-dependent photolysis in the visible range. A band filter, $280 \leq \lambda \leq 360$ nm, was used for ultraviolet photolysis. Iron was normally vaporized between 1300 and 1450 °C. The temperature of the cell was measured with a micro-optical pyrometer. Ultra pure iron (99.9985%) was obtained from Johnson Mathey, Inc. Matheson research grade argon (99.9995%) and ethylene (99.98%) were used without further purification. Enriched samples of $^{13}C_2H_4$ and $C_2D_4$ were purchased from U.S. Services, Inc. and KOR Isotopes with isotopic purities of 92% and 99%, respectively. Frequencies were measured to an accuracy of ±0.05 cm$^{-1}$.

## Results

The Fourier transform infrared spectra, obtained from iron/ethylene reaction products isolated in cryogenic matrices, were

(21) Swope, W. C.; Schaeffer, H. F., III *Mol. Phys.* **1977**, *34*, 1037.
(22) Basch, H.; Newton, M. D.; Moskowitz, J. W. *J. Chem. Phys.* **1978**, *69*, 584.
(23) Garcia-Prieto, J.; Novaro, O. *Mol. Phys.* **1980**, *41*, 205.
(24) Cohen, D.; Basch, H. *J. Am. Chem. Soc.* **1983**, *105*, 6980.
(25) Dewar, M. J. S. *Bull. Soc. Chim. Fr.* **1951**, *18*, 79.
(26) Chatt, J.; Duncanson, L. A.; *J. Chem. Soc.* **1953**, 2939.
(27) Hauge, R. H.; Fredin, L.; Kafafi, Z. H.; Margrave, J. L. *Appl. Spectrosc.*, submitted.
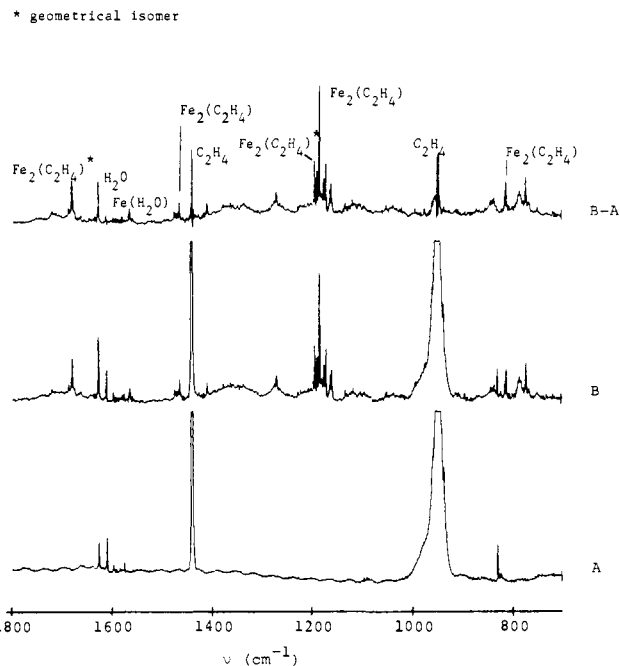
* geometrical isomer



**Figure 1.** A. Infrared spectrum of matrix-isolated ethylene in argon. Molar ratio of ethylene to argon $\simeq$ 5:1000. B. Infrared spectrum of matrix-isolated iron/ethylene in argon. Molar ratio of $Fe:C_2H_4:Ar \simeq$ 15:5:1000. Period of deposition = 30 min. Absorbance of strongest product peak = 0.08. Resolution = 1 cm$^{-1}$.

complicated and seemed quite puzzling at first. Many different experiments were initiated in order to understand the chemistry and unravel the types of interactions that took place between atomic and molecular iron and ethylene molecule(s) in inert gas matrices. Iron and ethylene concentration studies were undertaken to determine the stoichiometry of the different iron/ethylene complexes formed in the matrices. These various experiments made full use of the new multisurface matrix isolation apparatus recently developed in this laboratory.[27] The iron concentration was varied with respect to argon from part(s) per ten thousand to part(s) per hundred while that of ethylene was changed between part(s) per thousand to part(s) per hundred. Broad-band irradiation experiments in the visible and in the ultraviolet regions were carried out to verify and confirm some of the conclusions reached from the concentration studies as well as to study the photochemistry of the iron/ethylene system. Finally, experiments with carbon-13 and deuterium-labeled ethylene followed to confirm the bands and mode assignments for various products obtained either spontaneously or photolytically.

When iron was cocondensed with ethylene in excess argon, product bands appeared mainly in the 700–1800 cm$^{-1}$ region of the infrared spectrum. Figure 1 shows spectra obtained from typical deposition experiments. One must note that the intensities of the product bands are very weak; the strongest feature at 1182.9 cm$^{-1}$ has an absorbance of 0.08 for this highly concentrated matrix (Fe:Ar ~ 15:1000). Bands due to free ethylene, water, water iron complexes,[28] and possibly an iron cluster hydride[29] were observed (Figure 1a). This molecular hydride species absorbing at 1269.4 cm$^{-1}$ is thought to be formed as a result of the reaction between an iron cluster and residual molecular hydrogen present in the system. Product absorption bands were located in three main regions: 1400–1500 cm$^{-1}$, 1100–1300 cm$^{-1}$, and 700–900 cm$^{-1}$. These three regions are characteristic of the $\nu$(C=C) stretching, $\delta(CH_2)$ symmetric deformation, and $\rho_w(CH_2)$ wagging modes of transition-metal–olefin $\pi$-complexes.

Only one product absorption band appeared at 2988.2 cm$^{-1}$ in the $CH_2$ symmetric stretching region. The presence of this ab-

(28) Kauffman, J. W.; Hauge, R. H.; Margrave, J. L. *J. Phys. Chem.* **1985**, *89*, 3541.
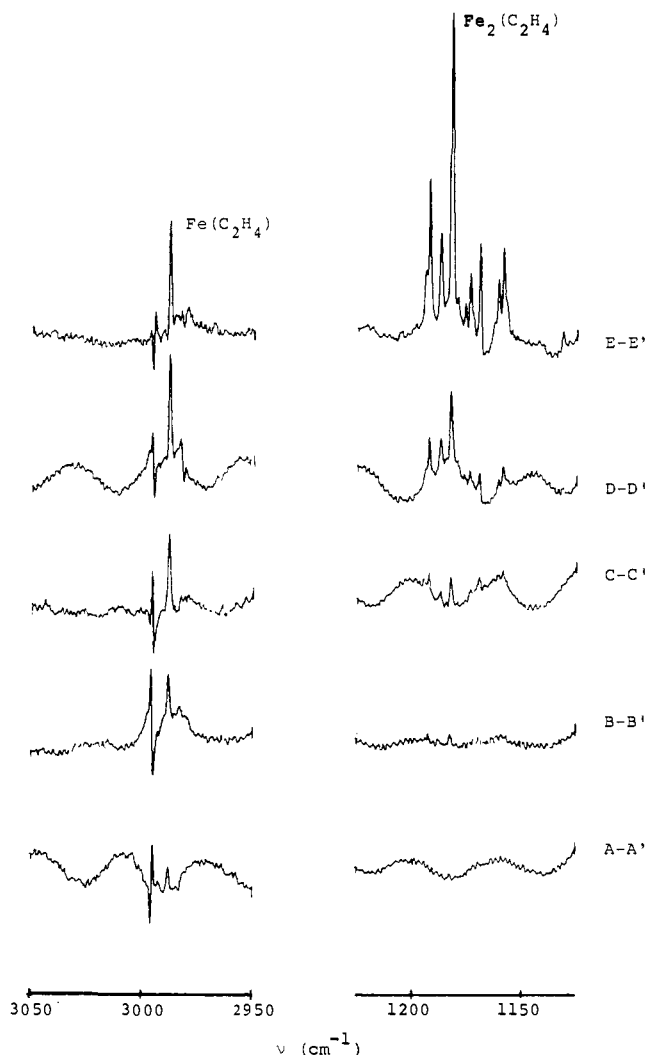(29) Kafafi, Z. H.; Hauge, R. H.; Margrave, J. L., unpublished results.

7552 *J. Am. Chem. Soc., Vol. 107, No. 25, 1985*

*Kafafi et al.*



Figure 2. An iron concentration study. FTIR difference spectra of $Fe/C_2H_4$ and $C_2H_4$ in Ar. Molar ratios for ($Fe:C_2H_4:Ar$): A, 0.2:6.8:1000; B, 0.4:7.0:1000; C, 1.1:6.9:1000; D, 2.2:7.9:1000; E, 7.7:4.9:1000. Molar ratios for ($C_2H_4:Ar$): A', 6.8:1000; B', 7.0:1000; C', 6.9:1000; D', 7.9:1000; E', 4.9:1000.

sorption was not obvious in the early experiments, and only after a careful metal concentration study were we able to observe definitively the rate of growth of this band as a function of iron concentration as depicted in Figure 2. It was necessary to go to much lower metal concentrations in the part(s) per ten thousand region, in order to see the development of this band as a function of iron concentration. Figure 2 shows the growth of this peak as well as the group of bands in the 1150–1250 cm$^{-1}$ region when the metal concentration was varied from 0.2 to 8 parts per thousand argon. Note that these are difference spectra where the ethylene peaks have been subtracted out. If one follows the growth of the 2988.2-cm$^{-1}$ peak, one notices that it appears in the most dilute matrix, varies linearly as a function of iron concentration, and reaches saturation around an iron concentration of two parts per thousand. At this metal dispersion the peaks in the $\delta(CH_2)$ deformation region pick up in intensity and continue to grow until a metal concentration of two parts per hundred is attained. On the basis of this metal concentration study, the peak at 2988.2 cm$^{-1}$ was assigned to an ethylene–iron complex whereas the other absorptions were identified with the diiron–ethylene complexes.

The photolytic behavior of the ethylene–iron complex may be followed in Figure 3. A decrease in the intensities of the $Fe(C_2H_4)$ and $C_2H_4$ absorption bands was observed upon visible photolysis ($\lambda \geq 400$ nm) with the growth of new adduct features at 2974.7 and 3088.0 cm$^{-1}$, respectively. UV ($280 < \lambda < 360$ nm) photolysis caused the reduction of all adduct peaks. New product features grew in at 2901.6, 2923.1, and 2999.5 cm$^{-1}$, respectively. Repeated
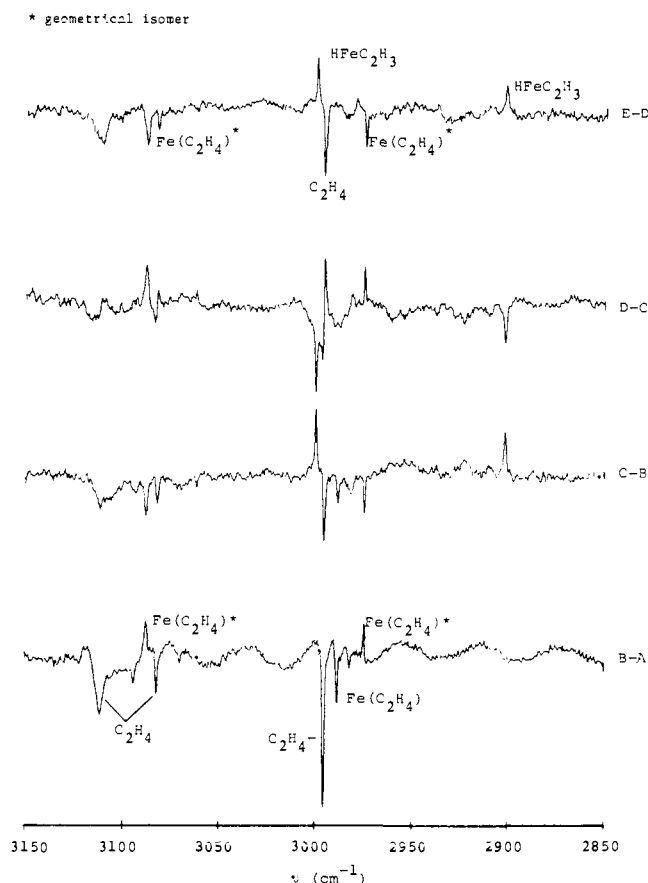


Figure 3. A reversible photolysis study. FTIR difference spectra of the carbon–hydrogen stretching region of $Fe/C_2H_4$ in Ar: A, no photolysis; B, $\lambda > 400$ nm, 20 min; C, 280 nm $< \lambda <$ 360 nm, 10 min; D, $\lambda > 400$ nm, 20 min; E, 280 nm $< \lambda <$ 360 nm, 10 min.

photolysis with $\lambda \geq 400$ nm caused the disappearance of these new bands and the reappearance of the adduct absorptions located at 2974.7 and 3088.0 cm$^{-1}$; a second photolysis in the ultraviolet resulted in the return of the new product features. In the iron-hydride stretching region depicted in Figure 4, an intense peak grew in with UV light and disappeared with $\lambda \geq 400$ nm irradiation. Repeated UV photolysis caused the reappearance of the photoproduct peak located at 1696.6 cm$^{-1}$. A large deuterium shift of the order of 476.1 cm$^{-1}$ was measured for this band. Other absorptions associated with the UV photoproduct were measured in the 450–4000 cm$^{-1}$ infrared spectral region. An iron–carbon stretching frequency was measured at 507.2 cm$^{-1}$ with a carbon-13 shift of 11.6 cm$^{-1}$. A C=C stretching frequency was also identified at 1556.3 cm$^{-1}$ with a 33.8-cm$^{-1}$ carbon-13 shift. Other ethylene-like frequencies measured in the $CH_2$ stretching and deformation modes showed typical deuterium isotopic shifts. The infrared spectrum of this molecular species indicates the presence of an iron—hydrogen, an iron—carbon, and a C=C double bond as well as an ethenyl moiety. We have thus identified it as vinyliron hydride, formed as a result of the UV rearrangement of the iron–ethylene adduct absorbing at 2974.7 and 3088.0 cm$^{-1}$. This adduct, photolytically ($\lambda \geq 400$ nm) formed, appears to be the necessary precursor for the photoinsertion product.

Close inspection of the iron-hydride or deuteride stretching region in Figure 5a reveals the presence of an absorption at 1660.7 cm$^{-1}$ which has been labeled iron dihydride. This frequency has been recently measured[30] in our laboratory in the photoreaction between atomic iron and hydrogen in solid argon. The infrared spectrum of $FeH_2$ has also been previously identified[31] in krypton

(30) Kafafi, Z. H.; Hauge, R. H.; Margrave, J. L., unpublished results.
(31) Ozin, G. A.; McCaffrey, J. G. *J. Phys. Chem.* **1984**, *88*, 645.
(32) Cowieson, D. R.; Barnes, J. A.; Orville-Thomas, W. *J. J. Raman Spectrosc.* **1981**, *10*, 224.
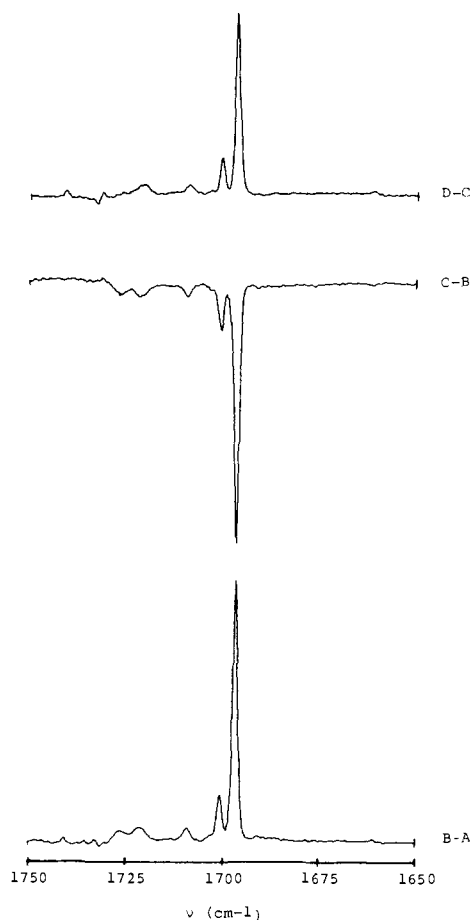(33) Duncan, J. L.; Hamilton, E. *J. Mol. Spectrosc.* **1981**, *76*, 65.

**Figure 6.** An ethylene concentration study. The $\nu(C{=}C)$ stretching and $\delta(CH_2)$ symmetric deformation regions of iron/ethylene $\pi$-complexes. Molar ratio of Fe:Ar $\simeq$ 6:1000. Molar % of $C_2H_4$ in Ar: $A = 0.5$, $B = 2.0$, $C = 5.0$, and $D = 12.0$.

Frequencies as high as 1745.0 cm$^{-1}$ and as low as 1660.9 cm$^{-1}$ were measured for the new absorption bands. This interesting annealing behavior may be explained in terms of the formation of different isomers of vinyliron hydride.

The results of the ethylene concentration study depicted in Figure 6 were used to determine the number of ethylene molecules present in the various iron/ethylene $\pi$-complexes. Initially bands due to $Fe_2(C_2H_4)$ were observed under the lowest ethylene concentration ($C_2H_4$:Ar $\sim$ 5:1000). The 1187.5-cm$^{-1}$ absorption grew at a faster rate than the 1182.9-cm$^{-1}$ peak and thus was assigned to $Fe_2(C_2H_4)_2$. The absorption band at 1221.4 cm$^{-1}$ showed the highest growth rate as a function of ethylene concentration. It was the only absorption band observed in the 1100–1300 cm$^{-1}$ region in a neat matrix. Furthermore, the results of the mixed $C_2H_4/^{13}C_2H_4$ isotopic study shown in Figure 7 clearly demonstrate that this complex has more than one ethylene. This band was assigned to diethylene–iron. However, one should not ignore the possibility that this absorption peak might be due to $Fe(C_2H_4)_n$ where $n > 2$ since intermediate complexes might be less stable and not spectroscopically observable. Nevertheless, for simplicity, the formula of this complex will be given as $Fe(C_2H_4)_2$ throughout the paper.

Figure 8 reflects spectral changes occurring as a function of ultraviolet photolysis time. Note that the ethylene concentration was quite high in this study. The $Fe(C_2H_4)_2$ absorption band initially increased with UV photolysis. Prolonged ultraviolet irradiation led to the increase in the intensity of the 1465.9-, 1374.5-, and 1305.1-cm$^{-1}$ bands and the decrease of the diethylene–iron peaks. No intensity change in the ethylene peak was detected. The absorptions at 1465.9 and 1374.5 cm$^{-1}$ belong to ethane, whereas the absorption at 1305.1 cm$^{-1}$ is due to methane. Thus it seems that ultraviolet photolysis ultimately leads to the disproportionation of the $\pi$-complex to possibly iron carbide, ethane, and methane.

Figure 9 shows a metal concentration study in the $\delta(CH_2)$ region for diiron–ethylene $\pi$-complexes in argon and krypton matrices. All the bands showed similar metal concentration dependence and could not be sorted out based on this particular study. However, the spectra obtained in solid krypton were rather simplified, due to the great reduction in intensity of the absorption bands present at 1194.2, 1192.5, 1161.2, and 1159.0 cm$^{-1}$ in an argon matrix. One is led to believe that there are at least two geometrical isomers of $Fe_2(C_2H_4)$ that have absorption bands at different frequencies, and krypton matrices favor the formation of one particular geometry.



**Figure 4.** A reversible photolysis study. FTIR difference spectra of the $\nu(Fe{-}H)$ region of matrix-isolated vinyliron hydride: A, $\lambda > 400$ nm, 20 min; B, 280 nm $< \lambda < 360$ nm, 60 min; C, $\lambda > 400$ nm, 20 min; D, 280 nm $< \lambda < 360$ nm, 100 min.



**Figure 5.** (a) The $\nu(FeH)$ and $\nu(FeD)$ regions for $HFeC_2H_3$ and $DFe$-$C_2D_3$, respectively. Molar ratios: Fe:$C_2H_4$:Ar $\simeq$ 10:5:1000 and Fe:$C_2D_4$:Ar $\simeq$ 8:4:1000. (b) The $\nu(FeH)$ region for $HFeC_2H_3$. Molar ratios of Fe:$C_2H_4$:Ar $\sim$ 1.5:7.8:1000: A, before annealing at 15 K; B, after annealing to 23 K; C, after annealing to 30 K.

and xenon matrices by Ozin and McCaffrey. Several weak bands associated with the strongest features at 1696.6 and 1220.5 cm$^{-1}$ assigned to $HFeC_2H_3$ and $DFeC_2D_3$, respectively, are also depicted in Figure 5a. These related frequencies have $\nu(FeH)/\nu(FeD)$ ratios identical with the strong features. Upon annealing the matrix to 23 K (Figure 5b), the two strong peaks located at 1696.6 and 1700.7 cm$^{-1}$ were reduced, the 1740.7-cm$^{-1}$ peak totally disappeared, and a new small peak grew in at 1703.3 cm$^{-1}$. Further annealing to 30 K resulted in a dramatic change in the spectrum with the total loss of the strongest absorptions and the concomitant growth of new peaks located to its left and to its right.
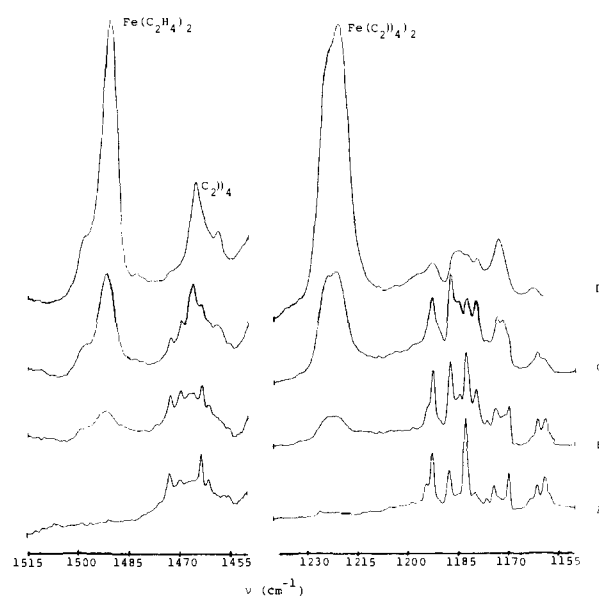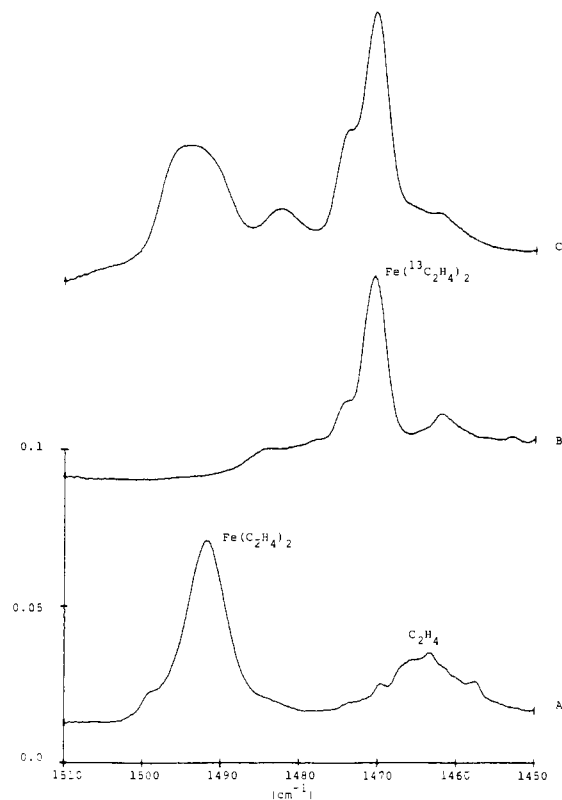
**Figure 7.** A mixed $C_2H_4/^{13}C_2H_4$ isotopic study. The $\nu(C{=}C)$ stretching region of iron/ethylene $\pi$-complexes. Molar ratio of Fe:$C_2H_4$:Ar $\simeq$ 9.5:52:1000: A, iron with $C_2H_4$ in argon; B, iron with $^{13}C_2H_4$ in argon; C, iron with $C_2H_4/^{13}C_2H_4$ in argon.
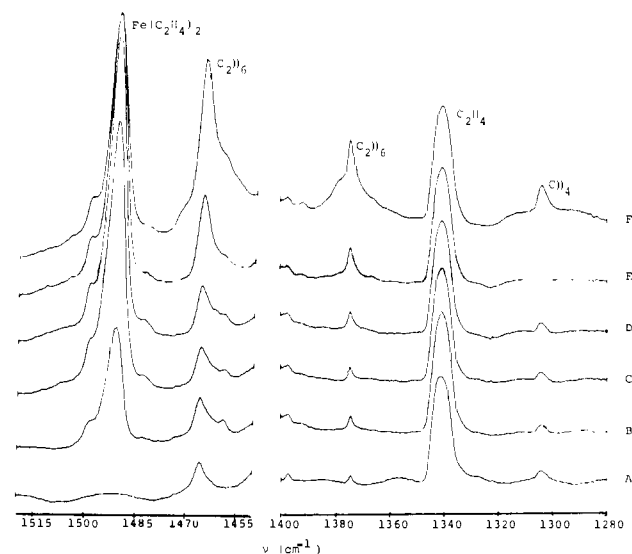


**Figure 8.** Time dependent photolysis study. The $\nu(C{=}C)$ stretching and the $\delta(CH_2)$ symmetric deformation regions of iron/etylene $\pi$-complexes. Molar ratio of Fe:$C_2H_4$:Ar $\simeq$ 6:124:1000: A, no iron; B, no photolysis; C, $\lambda \geq$ 400 nm, 20 min; D, 280 $< \lambda <$ 360 nm, 30 min; E, 280 $< \lambda <$ 360 nm, 4 h; F, 280 $< \lambda <$ 360 nm, 16 h.

Table I lists all the frequencies measured in the region below 2000 cm$^{-1}$ for product absorption bands of Fe/$C_2H_4$ in Ar and Kr and of Fe/$^{13}C_2H_4$ and Fe/$C_2D_4$ in Ar. Large carbon-13 isotopic shifts on the order of 20–30 cm$^{-1}$ were measured for $\nu(C{=}C)$ as well as $\delta_w(CH_2)$ modes of the different iron/ethylene $\pi$-complexes. Small carbon-13 shifts on the order of a few wavenumbers were measured for the $\rho_w(CH_2)$ wagging mode. A few bands located at 1676.6, 847.3, and 771.9 cm$^{-1}$ exhibited neither a carbon-13 nor a deuterium shift.

The band assignments given in Table I were deduced from various experiments whose results are presented in Figures 2, 6,
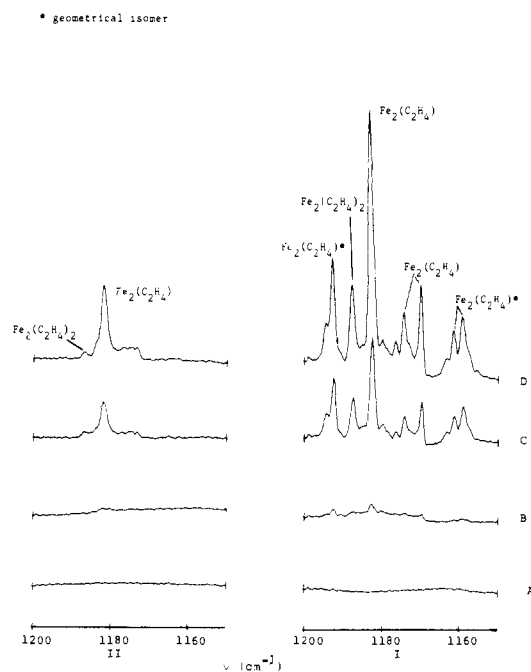


**Figure 9.** An iron concentration study. The $\delta(CH_2)$ symmetric deformation region of iron/ethylene $\pi$-complexes. Molar ratio of $C_2H_4$:Ar(1) or Kr(II) $\simeq$ 5:1000. Molar ratio of Fe:1000Ar; $A$ = 0, $B$ = 0.8, $C$ = 5.0, and $D$ = 15.0.

**Table I.** FTIR Frequencies (cm$^{-1}$) Measured for Iron/Ethylene Products in Solid Argon and Krypton

| Fe/$C_2H_4$ | | Fe/$^{13}C_2H_4$ | Fe/$C_2D_4$ | molecular |
|---|---|---|---|---|
| Kr | Ar | Ar | Ar | formula |
| | 1683.1 | | 1682.0 | $Fe_2(C_2H_4)$ |
| | 1676.6 | 1676.6 | 1675.6 | $Fe_2(C_2H_4)$ |
| | 1491.2 | 1470.5 | 1334.7 | $Fe(C_2H_4)_2$ |
| | | | 1329.7 | |
| 1472.6 | 1472.9 | 1455.8 | 1303.6 | $Fe_2(C_2H_4)$ |
| 1467.1 | 1466.1 | 1446.6 | 1295.4 | $Fe_2(C_2H_4)_2$ |
| 1460.6 | 1463.5 | 1439.8 | 1291.8 | $Fe_2(C_2H_4)$ |
| | 1461.3 | 1453.1 | 1287.5 | |
| | | | 1272.8 | $Fe_2(C_2H_4)$ |
| | 1455.3 | | 1263.9 | $Fe_2(C_2H_4)$ |
| 1405.6 | 1408.3 | | | $Fe_2(C_2H_4)$ |
| | 1221.4 | 1194.2 | 944.0 | $Fe(C_2H_4)_2$ |
| | 1194.4 | 1174.0 | | $Fe_2(C_2H_4)$ |
| 1192.3 | 1192.5 | 1170.3 | | $Fe_2(C_2H_4)$ |
| 1186.5 | 1187.5 | 1158.3 | 936.0 | $Fe_2(C_2H_4)_2$ |
| | 1184.6 | | | |
| 1181.9 | 1182.9 | 1153.7 | 933.1 | $Fe_2(C_2H_4)$ |
| | 1179.7 | 1149.4 | | $Fe_2(C_2H_4)_2$ |
| 1176.6 | 1176.4 | | | |
| 1173.2 | 1174.2 | 1145.5 | | $Fe_2(C_2H_4)$ |
| | 1173.0 | | | $Fe(C_2H_4)_2$ |
| | 1169.9 | 1140.0 | 929.5 | $Fe_2(C_2H_4)$ |
| | 1161.2 | | | $Fe_2(C_2H_4)$ |
| | 1159.0 | 1131.3 | | $Fe_2(C_2H_4)$ |
| 847.8 | 847.3 | | 847.8 | |
| 811.6 | 815.0 | 807.8 | | $Fe_2(C_2H_4)_2$ |
| 810.0 | 812.6 | 804.9 | 625.1 | $Fe_2(C_2H_4)$ |
| | 771.9 | 771.6 | 775.5 | |
| 746.8 | 748.0 | | | |

9, 10, and 11. The metal concentration study experiments (Figures 2 and 9), the ethylene concentration study experiments (Figure 6), and the mixed $C_2H_4/^{13}C_2H_4$ isotopic study experiments (Figure 7) carried out on the multisurface matrix isolation apparatus have already been discussed. The objective of these studies was to determine the molecular formulas of the different iron/ ethylene complexes formed in cryogenic matrices. Photolysis studies (Figures 10 and 11) were also undertaken to verify the band assignments of the different absorbing species and follow their photochemistry.
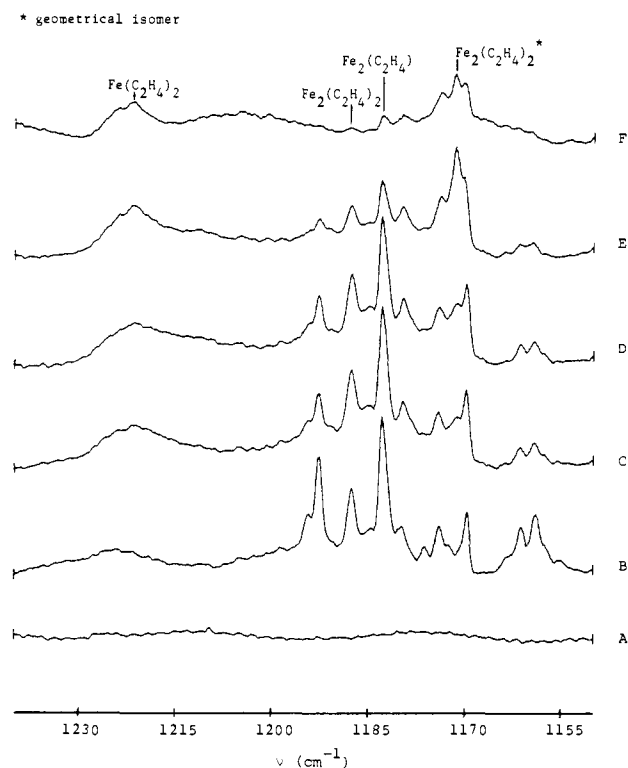
*FTIR Spectrum of Ethenyliron Hydride*

*J. Am. Chem. Soc., Vol. 107, No. 25, 1985* 7555



Figure 10. A time dependent photolysis study. The $\delta(CH_2)$ symmetric deformation region of iron/ethylene $\pi$-complexes. Molar ratio of Fe:$C_2H_4$:Ar $\simeq$ 4:8:1000; A, no iron; B, no photolysis; C, $\lambda \geq 400$ nm, 5 min; D, $280 < \lambda < 360$ nm, 5 s; E, $280 < \lambda < 360$ nm, 5 min; F, 280 $< \lambda < 360$ nm, 90 min.

The wavelength and time dependent photolytic study depicted in Figure 10 demonstrates the sensitivity of the 1194.2-, 1192.5-, 1161.2-, and 1159.0-cm$^{-1}$ bands to visible light ($\lambda \geq 400$ nm). A new absorption at 1171.5 cm$^{-1}$ started growing with visible irradiation and continued to do so with ultraviolet photolysis. The 1187.5- and 1182.9-cm$^{-1}$ peaks assigned to diethylene- and ethylene–diiron, respectively, were not sensitive to visible irradiation but started losing intensity with ultraviolet photolysis. Prolonged ultraviolet photolysis caused the disappearance of all bands with the exception of the 1171.5 cm$^{-1}$ and the diethylene–iron peaks. On the basis of their photolytic behavior, these peaks have been grouped into two sets and assigned to two geometrical isomers of $Fe_2(C_2H_4)$.

The 1171.5-cm$^{-1}$ peak showed an ethylene concentration dependence similar to the 1187.7-cm$^{-1}$ band belonging to diethylene–diiron. It was only present in matrices with high iron concentrations. A good candidate for this peak would be a geometrical isomer of $Fe_2(C_2H_4)_2$. A carbon-13 shift of 28.6 cm$^{-1}$ has been measured for this absorption compared to 29.2 cm$^{-1}$ for both $Fe_2(C_2H_4)$ (1182.9 cm$^{-1}$) and $Fe_2(C_2H_4)_2$ (1187.5 cm$^{-1}$) and to 22.2 cm$^{-1}$ for $Fe_2(C_2H_4)$ (1192.5 cm$^{-1}$).

Figure 11 represents spectra obtained from the cocondensation of iron with carbon-13 labeled ethylene in argon in a wavelength-dependent reversible photolytic study. Two bands at 1170.3 cm$^{-1}$ and at 1131.3 cm$^{-1}$ assigned to ethylene–diiron decreased in intensity with visible photolysis with a 500-nm cutoff filter. The effect of the shorter wavelength photolysis using the 400-nm cutoff filter on the $Fe_2(^{13}C_2H_4)$ bands was much more dramatic. The band at 1194.2 cm$^{-1}$ has shifted by 27.2 cm$^{-1}$ from its carbon-12 analogue and belongs to $Fe(^{13}C_2H_4)_2$. It started growing with visible photolysis and continued to do so with ultraviolet irradiation. The ethylene–diiron and diethylene–diiron bands were reduced upon exposure to UV light. Subsequent visible photolysis resulted in a small growth of the $Fe_2(C_2H_4)$ absorption band which was further reduced by a second exposure to ultraviolet light. This apparently reversible photolytic cycle was repeated several times and showed a small disappearance and reappearance of the ethylene–diiron absorption with ultraviolet (280 nm $\leq \lambda \leq$ 360
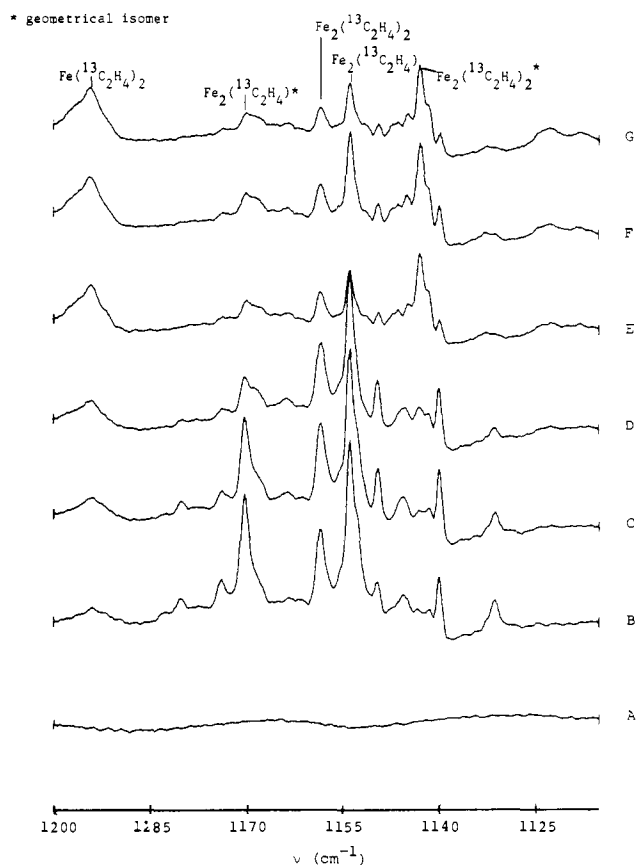


Figure 11. A reversible photolysis study. The $\delta(CH_2)$ symmetric deformation region of iron/ethylene $\pi$-complexes. Molar ratio of Fe:$^{13}C_2H_4$:Ar $\simeq$ 4:8:1000: A, no iron; B, no photolysis; C, $\lambda \geq 500$ nm, 20 min; D, $\lambda \geq 400$ nm, 20 min; E and G, $280 < \lambda < 360$ nm, 30 min; F, $\lambda \geq 400$ nm, 12 min.

nm) and visible ($\lambda \geq 400$ nm) broad band irradiation, respectively.

## Discussion

**I. Reaction of Atomic Iron with Ethylene.** Monatomic iron reacted with ethylene to form the ethylene–iron and the diethylene–iron complexes. The bonding between the metal atom and the alkene molecule in these two adducts was found, surprisingly, to be quite different. The interaction between atomic iron and ethylene is through one or more of its hydrogen(s). Thus, the infrared spectrum exhibited by this molecule is ethylene-like with only measurable perturbations in the $CH_2$ stretching region of ethylene. Furthermore, no large frequency shift typical of $\pi$-interaction was detected on the $\nu_2(C=C)$ frequency as deduced from the measured $\nu_2 + \nu_{12}$ combination band. The interaction of an iron atom with two ethylene molecules leads to the activation and large frequency shifts of the $\nu(C=C)$ stretching and the $\delta(CH_2)$ bending modes of ethylene, a spectrum characteristic of a metal atom $\pi$-coordinated to olefins.

The photolytic behavior of the two matrix-isolated mononuclear iron complexes has also proved to be different. Photolysis of $Fe(C_2H_4)$ in the near UV (280–360 nm) resulted in the photoinsertion of monatomic iron into one of the C–H bonds of ethylene forming ethenyliron hydride. Initial near UV photolysis increased the yield of the diethylene–iron complex. However, prolonged photolysis of $Fe(C_2H_4)_2$ caused its partial loss with apparent disproportionation to methane, ethane, and possibly iron carbide.

**(a) $Fe(C_2H_4)$.** Two geometrical isomers, A and B, of ethylene–iron have been isolated in an argon matrix. When iron vapors were cocondensed with ethylene in solid argon, complex A was formed. Photolysis with a 400-nm cutoff filter resulted in the disappearance of the IR bands associated with A and the formation of new absorptions assigned to complex B. Thus, it seems that complex A photolytically converts presumably to the more stable

**Table II.** FTIR Frequencies (cm$^{-1}$) Measured for Free Ethylene and the Hydrogen-Bonded Ethylene–Iron Complexes in Solid Argon

| vibrational mode for free ethylene | | Fe(C$_2$H$_4$) | Fe($^{13}$C$_2$H$_4$) | Fe(C$_2$D$_4$) |
|---|---|---|---|---|
| $\nu_9$, CH$_2$ or CD$_2$ a-stretch | E | 3112.1[d] | 3103.1 | 2345.7 |
| | A | 3106.0[e] | 3094.5 | 2340.2 |
| | B | 3088.0[f] | 3077.8, 3072.5 | 2328.6 |
| $\nu_2 + \nu_{12}$, C=C stretch | E | 3082.7 | 3052.3 | |
| + CH$_2$ scis | A | 3070.1 | 3044.1 | |
| | B | | 3033.0 | |
| $\nu_{11}$, CH$_2$ or CD$_2$ s-stretch | E | 2995.4 | 2974.4 | 2205.5 |
| | A | 2988.2 | 2967.4 | 2201.1 |
| | B | 2974.7 | 2955.9 | 2190.5 |
| $\nu_2$, C=C stretch | E | 1629[a] | 1587.6[b] | 1518.4[b] |
| | A | (1631.9)[c] | (1611.7)[c] | |
| | B | | (1603.5)[c] | |
| $\nu_{12}$, CH$_2$ or CD$_2$ scis | E | 1440.3 | 1434.8 | 1074.9 |
| | A | 1438.2 | 1432.4 | 1073.7 |
| | B | 1435.3 | 1429.5 | 1071.5 |
| $\nu_7$, CH$_2$ or CD$_2$ wag | E | 947.4 | 942.8 | 721.0 |
| | A | 947.4 | 942.8 | 718.6 |
| | B | 946.4 | 941.3 | 717.4 |

[a] Reference 32. [b] Reference 33. [c] From $\nu_2 + \nu_{12}$ and $\nu_{12}$. [d] E = C$_2$H$_4$. [e] A = Fe(C$_2$H$_4$), spontaneously formed. [f] B = Fe(C$_2$H$_4$), photolytically formed.

**Table III.** FTIR Frequencies (cm$^{-1}$) Measured for Ethenyliron Hydride

(a) In Solid Argon and Krypton

| approx type of vibrational mode | HFeC$_2$H$_3$ Kr | HFeC$_2$H$_3$ Ar | HFe$^{13}$C$_2$H$_3$ Ar | DFeC$_2$D$_3$ Ar |
|---|---|---|---|---|
| CH$_2$ or CD$_2$, a-stretch | | 2999.5 | 2987.2 | 2264.5 |
| CH or CD, stretch | 2913.0 | 2923.1 | 2921.6 | 2175.3 |
| CH$_2$ or CD$_2$, s-stretch | | 2901.6 | | 2150.5 |
| FeH or FeD, stretch | 1683.8 | 1696.6 | 1696.1 | 1220.5 |
| C=C, stretch | 1563.0 | 1556.3 | 1522.5 | 1477.4 |
| CH$_2$ or CD$_2$, sciss | 1408.3 | 1399.1 | 1359.1 | 1063.1 |
| CH$_2$ or CD$_2$, rock | 1020.9 | 1019.0 | 1016.1 | 713.5 |
| HCFe or DCFe, bend | 980.2 | 972.9 | 969.3 | |
| CH$_2$ or CD$_2$, wag | 944.7 | 944.2 | 934.6 | 737.4 |
| Fe–C, stretch | | 507.2 | 495.6 | 491.0 |

(b) In Argon Matrix before and after Annealing to 30 K[a]

| before annealing (15 K) | after annealing (30 K) |
|---|---|
| ... | 1745.0 |
| 1740.7 | ... |
| ... | 1735.6 |
| ... | 1726.0 |
| 1721.2 | ↓ |
| 1709.1 | ↑ |
| 1703.3 | ↑ |
| 1700.7 | ↓ |
| 1696.6 | ↓ |
| 1691.0 | ↑ |
| ... | 1686.9 |
| ... | 1682.3 |
| ... | 1674.9 |
| 1660.9 | ↑ |

[a] Key: ..., not present; ↓, decreased; ↑, increased.

complex B. Table II lists the frequencies measured for both geometrical isomers along with those for matrix-isolated free ethylene. Very small frequency shifts are exhibited by both forms of Fe(C$_2$H$_4$), reflecting the weakness of these complexes. The largest measured frequency shifts are for the carbon–hydrogen stretching frequencies, suggesting that this metal atom is interacting with one or more hydrogen atom(s) of ethylene. These shifts are of the order of 0.2% for complex A and 0.7% for complex B. Thus, the perturbations caused by the metal atom on the hydrogen atom(s) of ethylene are larger for complex B than complex A, resulting perhaps from a stronger interaction and possibly a more stable geometrical isomer. It is difficult to predict the geometrical configurations of these two complexes from the above experimental data. However, one may speculate about different possible structures as shown below:
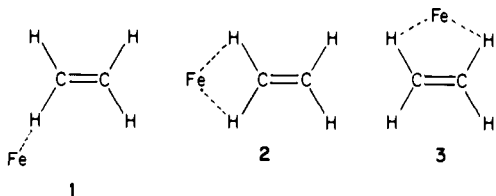


Only one of the hydrogen atoms of ethylene may interact with iron, resulting in **1**. The metal atom may also bond to two hydrogen atoms either end-on (**2**) or side-on (**3**). Other nonplanar configurations or geometries that include bonding of the metal atom to more than two hydrogen atoms are possible.

It is rather surprising that monoatomic iron coordinates to ethylene through the hydrogen atom(s) rather than the π-system of the C=C bond. However, theoretical calculations carried out by Swope and Schaeffer[21] on the neighboring atom, Mn, have suggested that Mn(C$_2$H$_4$) is at best weakly π-bound with an estimated dissociation energy of 0–11 kcal/mol compared to 14.2 kcal/mol calculated[6] for the more stable ethylene–nickel π-complex. The latter has been isolated in cryogenic matrices[8] and has shown thermal stability up to 35 K. Theoretical calculations regarding the stabilities of different possible structures of hydrogen-bonded vs. π-bonded zerovalent transition-metal complexes are needed to explain these experimental results. To the authors' knowledge, no theoretical investigation has yet addressed the question of a metal hydrogen bonding to an olefin.
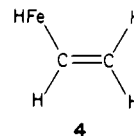
**(b) HFeC$_2$H$_3$. 1. Structure and Isomerism.** The photoexcitation of the ethylene–iron complex leads to insertion of the iron atom into one of the C–H bonds of ethylene, yielding ethenyliron hydride (**4**).



**4**

This molecule may have either $C_s$ or $C_1$ symmetry depending on whether the HFeC segment of the molecule is planar or nonplanar. In either case all 15 vibrational modes are infrared active, of which ten and seven frequencies have been measured in argon and krypton matrices, respectively. These frequencies are listed in Table III along with their analogues for HFe$^{13}$C$_2$H$_3$ and DFeC$_2$D$_3$.

The power of the technique of infrared matrix isolation spectroscopy as a diagnostic tool, in this case the only tool, has been clearly demonstrated in this study. The observation of the iron–hydrogen and iron–carbon stretching frequencies with their respective deuterium and carbon-13 shifts was crucial in the identification of the HFeC moiety, signaling the metal atom insertion into the C–H bond. The remainder of the spectrum had absorption in the stretching and bending mode regions of the CH$_2$ group and in the C=C stretching region characteristic of a vinyl functional group. Combining the HFeC with the vinyl skeleton results in the identification of the UV photoproduct as HFeC$_2$H$_3$, vinyliron hydride.

The iron–hydride stretching region shows small spectral features close to the main strong peak at 1696.6 cm$^{-1}$. These satellites are also associated with ethenyliron hydride. The annealing behavior of all the bands in this region indicated that this molecule is trapped in more than one configuration inside the argon cage. These different structures may arise from the rotation of the H–Fe bond around the Fe–C axis and thus could be identified as rotational conformers. Geometrical isomers may also be created as a result of a matrix-induced effect. In either case the presence of multiple conformers suggests low barriers to rotation about the Fe–C axis. Table IIIb lists the frequencies of the H–Fe stretch for the different configurations of vinyliron hydride measured

**Table IV.** FTIR Frequencies (cm$^{-1}$) Measured for the Isotopomers of the Diethylene–Iron $\pi$-Complex in Argon Matrix

| vibrational mode | $Fe(C_2H_4)_2$ | $Fe(^{13}C_2H_4)_2$ | $Fe(C_2D_4)_2$ |
|---|---|---|---|
| CH$_2$ or CD$_2$, a-stretch | 3052.3 | | |
| CH$_2$ or CD$_2$, s-stretch | 2974.2 | | |
| C=C, stretch | 1491.2 | 1470.5 | 1334.7, 1329.7 |
| | 1489.2$^a$ | | |
| CH$_2$, scis | 1221.4 | 1194.2 | 944.0 |
| | 1217.8$^a$ | | |

$^a$ Frequencies measured in neat ethylene matrix.

before and after annealing the matrix to 30 K.

**2. Oxidative-Addition/Reductive-Elimination.** An interesting photoreversibility effect exhibited by vinyliron hydride is indicated in eq 1. Upon excitation in the visible ($\lambda \geq 400$ nm) this insertion product rearranges back to the complex Fe(C$_2$H$_4$), isomer B; with UV photolysis it is partially regenerated. This sequence of alternate photolysis with UV and visible radiation may be repeated many times with the formation of vinyliron hydride and disappearance of isomer B of ethylene–iron and vice versa, respectively.

$$Fe(C_2H_4) \underset{\lambda > 400 \text{ nm}}{\overset{280–360 \text{ nm}}{\rightleftharpoons}} HFeC_2H_3 \qquad (1)$$
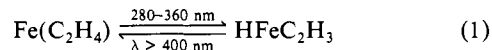
A similar oxidative-addition/reductive-elimination reaction has been previously demonstrated by Ozin et al.[34] for the Fe/CH$_4$ system. These authors have shown that irradiation with 420-nm light caused total bleaching of CH$_3$FeH with the generation of atomic iron as was reflected by the growth of the atomic resonance lines in the optical spectrum. On the other hand, narrow-band irradiation with 300-nm light caused the rapid disappearance of iron atoms with the growth of the bands in the infrared and optical spectra assignable to HFeCH$_3$. Kafafi et al.[35] have recently proved that it is the photoexcitation of the Fe(CH$_4$) adduct and not free iron atoms that leads to photoinsertion of atomic iron into the C–H bond of CH$_4$. Thus, in both instances the hydrogen-bonded complex Fe(CH$_4$) or Fe(C$_2$H$_4$) was shown to be the precursor for the photoinsertion of atomic iron into the C–H bond to form HFeCH$_3$ or HFeC$_2$H$_3$, respectively. Similar oxidative-addition/reduction-elimination reactions of atomic iron with propylene and ethane[36] have also been observed. A recent report by Bergman[37] on the thermal reaction between (C$_5$Me$_5$)-(PMe$_3$)(C$_6$H$_{11}$)(H)Ir and C$_2$H$_4$ has demonstrated the formation of a vinyliridium hydride complex (66% yield) as well as an iridium $\pi$-complex (34% yield). No interconversion between the $\pi$-complex and the vinylmetal hydride or vice versa was observed, suggesting that the $\pi$-complex is not a precursor for the formation of the C–H insertion product. These results imply that another type of complex is the precursor for the iridium insertion product. This complex was not isolated under the conditions of Bergman's experiments, possibly because of a low activation barrier for the metal C–H insertion. The technique of matrix isolation is known for its ability to isolate unstable reaction intermediates. This explains the success of the present study in observing the precursor for the iron photoinsertion product, namely the metal hydrogen-bonded ethylene complex, Fe(C$_2$H$_4$).

It is interesting, however, that photolysis of HFeC$_2$H$_3$ leads primarily to one particular isomer (complex B) of Fe(C$_2$H$_4$). This phenomenon may suggest that there is a well-defined reaction path where photoconversion of HFeC$_2$H$_3$ leads only to this isomeric form of Fe(C$_2$H$_4$) and vice versa. If one assumes that the most preferred geometry for Fe(C$_2$H$_4$) is **2**, one may speculate that upon UV excitation the iron atom is only partially bonded to the carbon and hydrogen, which then leads to the insertion product. This proposed mechanism seems reasonable since it naturally leads to a structure for vinyliron hydride similar to that reported for the isolated transition-metal vinylhydride complexes, vinyliridium

hydride[37] and vinylhafnium hydride.[38] A similar diagram may be drawn starting from structure **3** for Fe(C$_2$H$_4$).
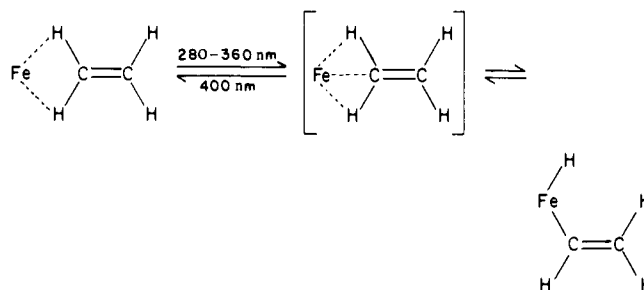


**(c) Fe(C$_2$H$_4$)$_2$.** Reaction of atomic iron with two ethylene molecules led to the formation of diethylene–iron. This complex exhibits an infrared spectrum characteristic of metal $\pi$-complexes. Its measured spectrum is very similar to that originally reported for Fe(C$_2$H$_4$).[2] The erroneous spectral assignment was partly due to the relatively high concentration of the substrate used in the reported study (molar ratio of C$_2$H$_4$:Ar on the order of 10–12%), which predominantly favored the formation of the diethylene–iron complex (see Figure 6D). In our experiments, the ethylene dispersion was lowered to 0.5% in order to eliminate totally the diethylene–iron products. Table IV lists the infrared frequencies measured for Fe(C$_2$H$_4$)$_2$ in argon and in neat matrices and for Fe($^{13}$C$_2$H$_4$)$_2$ and Fe(C$_2$D$_4$)$_2$ in an argon matrix. The activated C=C stretching frequency has red shifted by 138 cm$^{-1}$ from the free ethylene value, an 8% decrease. This mode is strongly coupled with the activated $\delta$(CH$_2$) scissoring mode. This is apparent from the large carbon-13 shift exhibited by the symmetric CH$_2$ bending mode. The measured $\delta$(CH$_2$) frequency is 122 cm$^{-1}$ lower than that of free ethylene, a 9% decrease in frequency. Since the $\nu$(C=C) and $\delta$(CD$_2$) modes do not mix substantially in the case of C$_2$D$_4$, the frequency shift of the $\nu$(C=C) mode of Fe(C$_2$D$_4$) from that of free C$_2$D$_4$ is a more accurate measure of the weakening of the C=C bond of ethylene as a result of $\pi$-coordination of the metal atom. This shift has been measured to be 183.7 cm$^{-1}$, a 12% decrease in frequency, reflecting a considerable loss of the double bond order of the ethylene carbon–carbon bond. In the case of the interaction of ethylene with the iron surface, the $\nu$(C=C) mode shows larger red frequency shifts, whereas the $\delta$(CH$_2$) scissor mode is not perturbed much. A study of ethylene chemisorbed on the Fe(110) surface[39] gives frequencies equal to 1250 cm$^{-1}$ for the carbon–carbon stretching and 1410 cm$^{-1}$ for the CH$_2$ scissor modes, respectively. It seems that $\pi$-d forward- and back-bonding interactions for chemisorption on a clean iron surface weaken and stretch the carbon–carbon bond of C$_2$H$_4$ to such an extent that the breaking of the C=C bond is induced in some cases.[40,41]

One may envision many possible structures for the diethylene–iron $\pi$-complex, two of which are shown below:
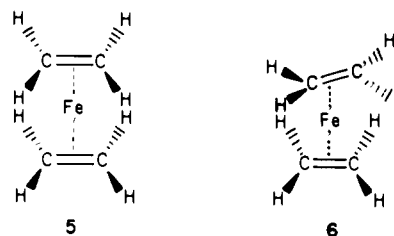


Rosch and Hoffmann[20] have calculated the total energies for structures **5** and **6** in the case of Ni(C$_2$H$_4$)$_2$. A marginal energy difference of 1.5 kcal/mol favoring the quasitetrahedral $D_{2d}$ configuration **6** was predicted.

(34) Ozin, G. A.; McCaffrey, J. G. *J. Am. Chem. Soc.* **1982**, *104*, 7351.
(35) Kafafi, Z. H.; Hauge, R. H.; Margrave, J. L. *J. Am. Chem. Soc.* **1985**, *107*, 6134.
(36) Kafafi, Z. H.; Hauge, R. H.; Margrave, J. L., unpublished results.
(37) Stoutland, P. G.; Bergman, R. G. *J. Am. Chem. Soc.* **1985**, *107*, 4581.

(38) Rodick, D. M.; Fryzuk, M. D.; Seidler, P. F.; Hillhouse, G. L.; Bercaw, J. E. *Organometallics* **1985**, *4*, 97.
(39) Erley, W.; Baro, A. M.; Ibach, H. *Surf. Sci.* **1982**, *120*, 273.
(40) Brucker, C.; Rhodin, T. *J. Catal.* **1977**, *47*, 214.
(41) Yoshida, K.; Somorjai, G. A. *Surf. Sci.* **1978**, *75*, 46.

Since $Fe(C_2H_4)_2$ was the only product formed in neat matrices, an experiment was conducted to determine its stability by allowing the matrix to warm up from 14 to 100 K. The absorptions due to $Fe(C_2H_4)_2$ lost half their intensity at $T = 50$ K and totally disappeared at $T = 75$ K. Ozin et al.[11] have measured the decomposition temperatures for the triethylene–nickel group π-complexes. They were 190, 273, and 300 K for $Pd(C_2H_4)_3$, $Ni(C_2H_4)_3$, and $Pt(C_2H_4)_3$, respectively. They found that this stability order for bonding of $C_2H_4$ to Pd, Ni, and Pt parallels the respective heats of absorption for the respective metals.

Ultraviolet photolysis of diethylene–iron initially led to an increase in its yield. However, prolonged photolysis of this π-complex caused its dissociation and the formation of methane and ethane. Recently Cardenas and Shevlin[42] cocondensed Fe atoms with $C_2H_4$ at 77 K and obtained primarily $C_2H_6$ (73%) after allowing the system to warm up to room temperature. They have explained the formation of ethane in terms of an iron hydride formed from an initial insertion of iron into a C–H bond which caused the reduction of ethylene. In our present study, warming up the neat matrix to 75 K caused the total dissociation of the diethylene–iron complex. No new products were detected.

## II. Reaction of Diatomic Iron with Ethylene.

Diiron reacted with ethylene to form the π-complexes $Fe_2(C_2H_4)$ and $Fe_2(C_2H_4)_2$. Two geometrical isomers have been isolated for each complex, resulting in rich and complex infrared spectra. Frequencies previously reported[2] for the ethylene diiron complex were measured and identified with the diethylene–diiron complex. Both isomeric forms of ethylene–diiron were formed spontaneously and were photolytically sensitive. Only one geometrical isomer of $Fe_2$-$(C_2H_4)_2$ was formed spontaneously. UV irradiation caused its depletion with the formation of a new geometrical isomer.

**(a) $Fe_2(C_2H_4)$.** Contrary to the metal–hydrogen bonding exhibited by $Fe(C_2H_4)$, the bonding between diiron and ethylene is as expected between the metal dimer and the C=C π-system. The formation of $Fe_2(C_2H_4)$ π-complexes in spite of the absence of their mononuclear analogues may be explained in terms of the higher stability of the diiron adduct. Calculations carried out[6] on the $Ni/C_2H_4$ complexes predicted bond energies of 14.2 and 27.2 kcal/mol for $Ni(C_2H_4)$ and $Ni_2(C_2H_4)$, respectively. In the case of the metal dimer bonded to ethylene as shown in **7**, the metal atom may be withdrawing electron density from the metal atom π-bonded to ethylene, making the latter a better electron acceptor for the $C_2H_4$ π-electrons and thus strengthening the π-interaction. In this configuration the ethylene molecule was found to lose its planarity[6,22] by only a couple of degrees.
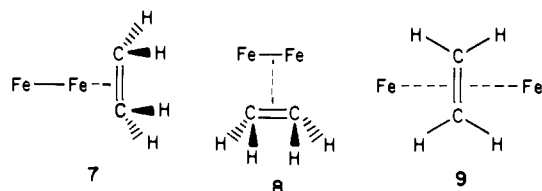


Another possible geometry for $Fe_2(C_2H_4)$ is depicted in **8** where the metal dimer is bridging the C=C π-orbital. One may refer to **7** and **8** as end-on and side-on (with respect to the metal) π-coordination. Finally, one may consider the π-coordination of two iron atoms to the ethylene C=C bond to produce a planar "di-π" complex such as **9**.

Table V lists the measured FTIR frequencies for the two matrix-isolated geometrical isomers of $Fe_2(C_2H_4)$, which will be referred to as isomer A and isomer B. The former exhibited smaller carbon-13 shifts than the latter, namely 22.2 cm$^{-1}$ vs. 29.2 cm$^{-1}$ for δ(CH$_2$) and 17.1 cm$^{-1}$ vs. 23.7 cm$^{-1}$ for ν(C=C). These two modes are highly coupled, as reflected by their large carbon-13 shifts. Thus, they are indistinguishable as far as specific modes assignment is concerned. Besides absorption bands due to the symmetric CH$_2$ bending and C=C stretching modes, isomer B exhibited a peak at 812.6 cm$^{-1}$ with a large deuterium shift of

---

(42) Cardenas, G.; Shevlin, P. B. *J. Org. Chem.* **1984**, *49*, 4726.

**Table V.** FTIR Frequencies (cm$^{-1}$) Measured for Ethylene–Diiron Complexes in Argon and Krypton Matrices

| Kr $Fe_2(C_2H_4)$ | Ar | | |
|---|---|---|---|
| | $Fe_2(C_2H_4)$ | $Fe_2(^{13}C_2H_4)$ | $Fe_2(C_2D_4)$ |
| isomer A | | | |
| | 1676.6 | 1676.6 | 1675.6 |
| 1472.6 | 1472.9 | 1455.8 | 1303.6 |
| | 1455.3 | | |
| | 1194.2 | 1174.0 | |
| 1192.3 | 1192.5 | 1170.3 | |
| | 1161.2 | | |
| | 1159.0 | 1131.3 | |
| isomer B | | | |
| 1460.6 | 1463.5 | 1439.8 | 1291.8 |
| | 1461.3 | | 1287.5 |
| | | | 1272.8 |
| 1181.9 | 1182.9 | 1153.7 | 933.1 |
| 1176.6 | 1176.4 | | |
| | 1174.2 | 1145.5 | |
| | 1169.9 | 1140.0 | 929.5 |
| 810.0 | 812.6 | 804.9 | 625.1 |

**Table VI.** FTIR Frequencies (cm$^{-1}$) Measured for Diethylene–Diiron Complexes in Argon and Krypton Matrices

| Kr $Fe_2(C_2H_4)$ | Ar | | |
|---|---|---|---|
| | $Fe_2(C_2H_4)$ | $Fe_2(^{13}C_2H_4)_2$ | $Fe_2(C_2D_4)_2$ |
| isomer A[a] | | | |
| 1467.1 | 1466.1 | 1446.6 | 1295.4 |
| 1186.1 | 1187.5 | 1158.3 | 936.0 |
| | 1180.0 | 1149.4 | |
| | 815.0 | 807.8 | |
| isomer B[b] | | | |
| | 1457.7 | | 1279.1 |
| 1173.2 | 1171.5 | 1142.9 | 924.6 |

[a] Isomer A, $Fe_2(C_2H_4)_2$, spontaneously formed. [b] Isomer B, $Fe_2(C_2H_4)_2$, photolytically formed.

187.5 cm$^{-1}$. This frequency was assigned to the CH$_2$ wagging mode of this complex.

An interesting absorption for isomer A appeared at 1676.6 cm$^{-1}$ with zero and one wavenumber carbon-13 and deuterium shifts, respectively. The lack of either a carbon-13 or a significant deuterium shift strongly suggests that it is due to an electronic transition of this complex. This is the first time such a d–d "forbidden" transition has been reported for a diatomic metal in the infrared region. In the absence of ethylene, this absorption was not present, suggesting the activation of this transition is caused by the perturbation of the ethylene molecule.

The photolytic behavior of both isomers was quite different. Isomer A was photolyzed away upon irradiation in the visible, λ > 500 nm. However, no photoproducts were observed. This behavior suggests simple photodissociation of $Fe_2(C_2H_4)$ to $Fe_2$ and $C_2H_4$. Isomer A may be forming as a result of the reaction of ethylene with $Fe_2$ on the matrix surface during the cocondensation experiment. Either structure **7** or **8** would be a possible candidate for isomer A where the metal is either end-on or side-on π-coordinated to ethylene. The fact that this complex absorbs in the visible spectrum is further support that the interaction is between an iron dimer rather than two iron atoms and ethylene. Shorter wavelength light was required to reduce isomer B absorptions. Photolysis in the visible did cause a small regeneration of the isomer B spectrum which could be removed by further photolysis with ultraviolet light. A repeat of the photolysis with λ > 400 nm caused the formation of a small amount of the same complex. Structure **9** may be a good candidate for isomer B since it absorbs light of shorter wavelength and thus acts more like a mononuclear iron ethylene adduct species. Thus isomer B may be formed by a sequential addition of atomic iron to ethylene whereas isomer A is produced by the reaction of diatomic iron and ethylene. Photolysis in the ultraviolet may cause the ejection of one iron atom from $Fe_2(C_2H_4)$ whereas irradiation in the visible (λ > 400 nm) may favor the recombination of Fe and $Fe(C_2H_4)$

to form the dinuclear iron ethylene adduct.

**(b) Fe$_2$(C$_2$H$_4$)$_2$.** Table VI lists the infrared frequencies measured for the diethylene–diiron complex. The spectrum exhibited by this complex is again characteristic of a $\pi$-complex. Two isomeric forms of Fe$_2$(C$_2$H$_4$)$_2$, denoted as isomer A and isomer B, have been matrix isolated. Isomer A was formed spontaneously upon the cocondensation of iron with ethylene in excess argon. Upon photolysis in the UV the absorptions due to A diminished with the concomitant growth of peaks at lower frequency, suggesting photoisomerization taking place from A to B. It is interesting that the spectra exhibited by Fe$_2$(C$_2$H$_4$), B, and Fe$_2$-(C$_2$H$_4$)$_2$, A, are very similar. Furthermore, their carbon-13 and deuterium shifts are extremely close, suggesting very similar structures.

## Summary of Results

1. A new type of interaction between a metal atom and an olefin has been demonstrated in this study. Monatomic iron is found to hydrogen bond to ethylene in two distinct forms. One of these forms was shown to be a necessary precursor for the formation of the insertion product, vinyliron hydride. An oxidative-addition/reductive-elimination reaction, which is photoreversible, has been observed:

$$Fe(C_2H_4) \underset{\lambda > 400 \text{ nm}}{\overset{280-360 \text{ nm}}{\rightleftharpoons}} HFeC_2H_3$$
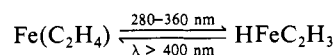
i.e., interconversion of ethylene iron to vinyliron hydride and vice versa.

2. The complexes Fe(C$_2$H$_4$)$_2$, Fe$_2$(C$_2$H$_4$), and Fe$_2$(C$_2$H$_4$)$_2$ have been isolated in argon and krypton matrices. Only Fe(C$_2$H$_4$)$_2$ was observed in neat ethylene matrices. The interaction between the metal and the olefin in this system follows the Dewar–Chatt–Duncanson model where the ethylene acts as a $\sigma$-donor through the (C=C) $\pi$-orbital and a $\pi$-acceptor through the (C=C) $\pi^*$ orbital. Photoexcitation of these $\pi$-complexes did not lead to the C–H activation of ethylene.

3. A d–d "forbidden" transition of Fe$_2$ has been observed for the first time in the infrared region. The activation of this electronic transition is the result of the complexation of the metal dimer to ethylene. A very small deuterium shift, 1 cm$^{-1}$, has been measured, which is a further proof of its assignment to a Fe$_2$(C$_2$H$_4$) complex.

# Matrix-Isolation Studies of the Reactions of Iron Atoms and Iron Dimers with Acetylene in an Argon Matrix. The FTIR Spectrum of Ethynyliron Hydride

**Ellen S. Kline, Zakya H. Kafafi,\* Robert H. Hauge, and John L. Margrave**

*Contribution from the Department of Chemistry and Rice Quantum Institute, Rice University, Houston, Texas 77251. Received May 13, 1985*

**Abstract:** The reactions of acetylene with iron vapors in argon matrices at 15 K have been investigated with Fourier-transform infrared spectroscopy. These studies indicated that at very low concentrations of acetylene and iron the monoiron–acetylene adduct, Fe(C$_2$H$_2$), was formed. The metal is found to be bonded through one of the hydrogen atoms of acetylene. This hydrogen-bonded complex rearranges upon near-ultraviolet photolysis to give ethynyliron hydride, HFeC$_2$H. At higher iron concentrations a diiron adduct, Fe$_2$(C$_2$H$_2$), is formed where the iron molecule is $\pi$-coordinated to acetylene. Studies with carbon-13 acetylene and deuterated acetylene support these findings.

The role of transition metals, particularly iron, in heterogeneous catalytic processes is of great interest. The structure and bonding of small molecules to transition metals have been extensively investigated with use of metal surfaces and metal cluster chemistry.[1-16] In particular, the interactions of acetylene with iron surfaces have been studied with new surface science techniques.[17-19] It has been postulated that the bonding patterns for unsaturated hydrocarbons in metal cluster chemistry are relatively similar to those found on transition-metal surfaces;[19-20] thus, mono- and

(1) Koestner, R. J.; Van Hove, M. A.; Somorjai, G. A. *J. Phys. Chem.* **1983**, *87*, 203-213.
(2) Dubois, L. H.; Castner, D. G.; Somorjai, G. A. *J. Chem. Phys.* **1980**, *72*, 5234-5240.
(3) Baetzold, R. C. *Surf. Sci.* **1980**, *95*, 286-298.
(4) Foulias, S. D.; Rawlings, K. J.; Hopkins, B. J. *Chem. Phys. Lett.* **1979**, *68*, 81-85.
(5) Kesmodel, L. L.; Dubois, L. H.; Somorjai, G. A. *J. Chem. Phys.* **1979**, *70*, 2180-2188.
(6) Demuth, J. E. *Surf. Sci.* **1979**, *80*, 367-387.
(7) Demuth, J. E. *Surf. Sci.* **1980**, *93*, 127-144.
(8) Gavezzotti, A.; Ortoleva, E.; Simonetta, M. *Theor. Chim. Acta* **1979**, *52*, 209-218.
(9) Muetterties, E. L.; Pretzer, W. R.; Thomas, M. G.; Beier, B. F.; Thorn, D. L.; Day, V. W.; Anderson, A. B. *J. Am. Chem. Soc.* **1978**, *100*, 2090-2096.

(10) Thorn, D. L.; Hoffmann, R. *Inorg. Chem.* **1978**, *17*, 126-140.
(11) Nelson, J. H.; Wheelock, K. S.; Cusachs, L. C.; Jonassen, H. B. *J. Am. Chem. Soc.* **1969**, *91*, 7005-7008.
(12) Tatsumi, K.; Fueno, T.; Nakamura, A.; Otsuka, S. *Bull. Chem. Soc. Jpn.* **1976**, *49*, 2170-2177.
(13) Wang, Y.; Coppens, P. *Inorg. Chem.* **1976**, *15*, 1122-1127.
(14) Carty, A. J.; Paik, H. N.; Ng, T. W. *J. Organomet. Chem.* **1974**, *74*, 279-288.
(15) Bailey, W. I., Jr.; Chisholm, M. H.; Cotton, F. A.; Rankel, L. A. *J. Am. Chem. Soc.* **1978**, *100*, 5764-5773.
(16) Wheelock, K. S.; Nelson, J. H.; Cusachs, L. C.; Jonassen, H. B. *J. Am. Chem. Soc.* **1970**, *92*, 5110-5114.
(17) Erley, W.; Baro, A. M.; Ibach, H. *Surf. Sci.* **1982**, *120*, 273-290.
(18) Yoshida, K.; Somorjai, G. A. *Surf. Sci.* **1978**, *75*, 46-60.
(19) Brucker, C.; Rhodin, T. *J. Catal.* **1977**, *47*, 214-231.